JOURNAL OF MOLECULAR SPECTROSCOPY **160,** 540–553 (1993)

The FT-IR Spectrum of $HC^{15}NO$: The ν_1, ν_2, $2\nu_3$, and $\nu_2 + \nu_3$ Band Systems

W. QUAPP,* S. ALBERT,† B. P. WINNEWISSER,† AND M. WINNEWISSER†

* *Mathematisches Institut, Universität Leipzig, Augustusplatz, O-7010 Leipzig, Germany; and*
† *Physikalisch-Chemisches Institut, Justus-Liebig-Universität, Heinrich-Buff-Ring 58, W-6300 Giessen, Germany*

The infrared spectrum of $HC^{15}NO$, an isotopically substituted species of fulminic acid, has been measured in the range 1900–3600 cm^{-1} at a resolution of 0.003 cm^{-1} with a Bruker IFS 120 HR interferometer. More than 100 subbands have been assigned. Power series coefficients for these transitions are given. A Coriolis resonance between the levels 01002 ($l = 0e$) and 01010 ($l = 1e$) allows normally "forbidden" transitions to occur, some of which were observed and assigned. We correlate transition intensities and energies of the resonance system. Variations in the manifold of $n\nu_5$ states with excitation of other modes are compared.

INTRODUCTION

The vibrational and rotational energy level structure of highly excited vibrational states in polyatomic molecules is currently of experimental and theoretical significance. The fulminic acid molecule, HCNO, is of interest because of its quasilinearity. It is important to obtain experimental data on its isotopomers in order to study the effects of isotopic substitution on the quasilinear HCN bending mode and also on the other bending degree of freedom and their interactions with the stretching modes. As there is now a relatively efficient synthesis (*1*), the investigation of the rovibrational spectra of $H^{13}CNO$, $HC^{15}NO$, and $H^{13}C^{15}NO$ is in progress. The rovibrational spectra in the far infrared have now been measured for HCNO and each of the above-mentioned isotopomers (*2–6*). Because of the low-lying quasilinear bending mode, the molecule offers a rich vibration–rotation overtone spectrum even below 4000 cm^{-1}. We are pursuing the observation and analysis of the spectrum to provide data for analysis of the anharmonic potential energy surface and for molecular dynamics studies of the full four-atomic molecule problem. One example is the analysis of the parent species by Iachello *et al.* (*7*) using the vibron model.

$HC^{15}NO$ has five normal modes, three stretching vibrations of Σ^+ symmetry, and two bending modes of II symmetry: ν_1 is the CH stretch at 3333.032 cm^{-1}, ν_2 is the CN stretch at 2152.014 cm^{-1}, and ν_3 is the NO stretch at 1251.218 cm^{-1}. The degenerate CNO bending mode ν_4 lies at 526.562 cm^{-1}, and the degenerate quasilinear HCN bending mode ν_5 at 223.417 cm^{-1}. The present results, covering the range 1900–3600 cm^{-1}, thus include the band systems ν_1, ν_2, $2\nu_3$, and $\nu_2 + \nu_3$.

For the present analysis of the data, we have used the formalism appropriate for a linear molecule (*3, 8*).

EXPERIMENTAL DETAILS

The ^{15}N substitution was introduced in the last step of the synthesis of 3-phenyl-4-oxoiminoisoxazol-*s*-(4*H*)-one (*1*), which was then pyrolyzed as in Ref. (*3*) to obtain

0022-2852/93 $5.00

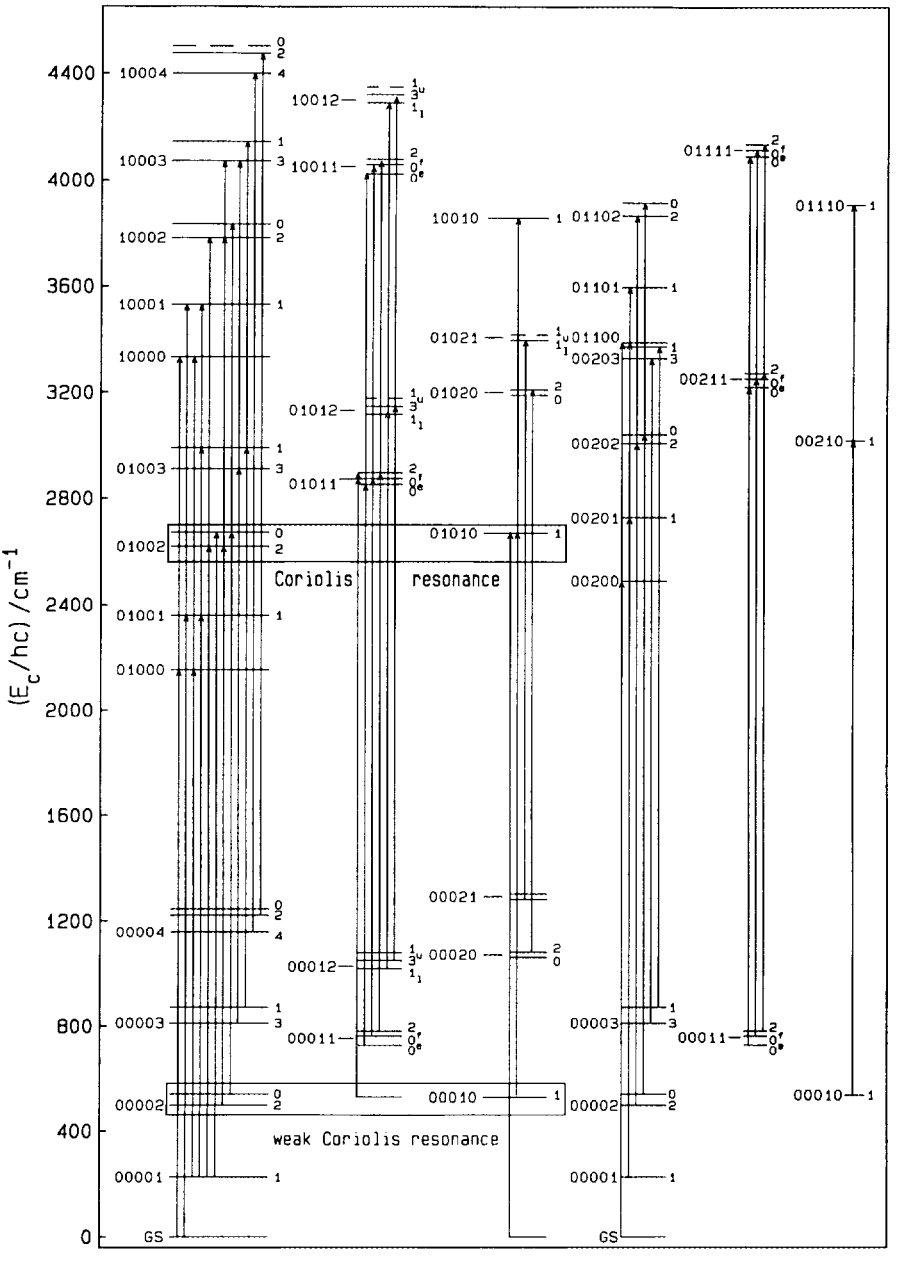

FIG. 1. Vibrational term diagram of HC[15]NO. The box near 2670 cm^{-1} indicates the strongest resonance.

HC[15]NO. The sample contained approximately 10% unsubstituted HCNO and small amounts of H[15]NCO and CO_2.

The experimental aspects are analogous to those described in Ref. (*3*). The cell length was 3 m, and the sample was swept into the cell and buffered with argon. The sample handling, as well as Fourier transformation, selection, summing, and obtaining of the transmittance spectra of [[15]N]fulminic acid were as in Ref. (*3*). The measure-

TABLE I

Band Centers and Lower States Power Series Constants of $HC^{15}NO$ in cm^{-1}, Taken from (*6*)

state	$\tilde{\nu}_c$	B_{ps}	D_{ps} $\times 10^7$	H_{ps} $\times 10^{12}$	L_{ps} $\times 10^{15}$
00000	-	0.382 536 85	1.418 61	-	-
00001^{1e}	223.416 585	0.382 958 78	1.401 4	-0.024	-
00001^{1f}	223.416 680	0.384 117 65	1.455 57	-	-
00002^{2e}	497.374 040	0.384 175 35	1.668 2	0.022	-
00002^{2f}	497.374 040	0.384 174 58	1.438 35	-0.088	-
00002^{0e}	540.160 581	0.384 031 26	1.210 75	-0.032	-0.0083
$0001^{1e}0$	526.561 639	0.382 663 40	1.419 1	0.407	-0.058
$0001^{1f}0$	526.561 639	0.383 410 70	1.436 7	0.156	-
$000(11)^{0e}$	747.111 034	0.384 056 4	4.467 0	1.1	18.5
$000(11)^{0f}$	748.897 029 3	0.383 989 67	1.840 6	-1.130	0.881
$000(11)^{2e}$	750.111 380	0.383 882 6	−1.952	-47.6	-
$000(11)^{2f}$	750.111 380	0.383 892 86	1.049 9	3.38	-1.790
00003^{3e}	811.002 450	0.384 848 33	1.558 3	-0.151	-
00003^{3f}	811.002 450	0.384 848 44	1.559 1	0.230	-
00003^{1e}	869.528 856	0.383 700 24	1.308 5	0.183	-
00003^{1f}	869.528 856	0.385 513 25	1.368 0	-0.188	-
00004^{0e}	1244.346 870	0.384 632 9	3.129	-92.0	-98.3
00004^{2e}	1221.742 292	0.385 126 3	2.313	1.16	-
00004^{2f}	1221.742 292	0.385 120 4	1.317 3	-	-
$00004^{4e,f}$	1157.813 319	0.385 257 2	1.555 3	-	-
00100^{0e}	1251.217 5	0.381 294	2.47	614.0	-114.7
$000(12)^{3}$	1024.860 39	0.384 465 4	1.268	-	-
$000(12)^{1e}$	1020.370 53	0.384 572	1.951	-	-
$000(12)^{1f}$	1020.369 88	0.384 771	1.877	-	-

ments were carried out in three regions, in each of which the resolution was chosen so that the full width at half height (FWHH) of the instrumental line shape was about one-half of the Doppler width. Thus, the resolution, given as the inverse of the maximum optical path difference, was 0.0033 cm^{-1} in the region of the optical band-pass 1850–2350 cm^{-1} and 0.0044 cm^{-1} in the band-pass 2300–3000 cm^{-1}. The latter two regions were calibrated with N_2O (*10*). The uppermost region, 3100–3600 cm^{-1}, was measured with a resolution of 0.0055 cm^{-1} and calibrated with HCN (*11*). There is a gap, in which no significant absorption is observed, between 3000 and 3100 cm^{-1}, which was not measured.

ASSIGNMENT AND ANALYSIS OF THE SPECTRUM

The vibrational transitions observed for $HC^{15}NO$ are summarized in Fig. 1 which displays the vibrational term diagram. The assignments were made initially in analogy with those of the parent species of HCNO (*12–14*) and confirmed using lower-state combination differences or by comparing the lower-state rotational parameters with those obtained in Refs. (*5, 6*). The observation of many vibrational states two or three times over, in transitions from the ground state and from various excited levels, confirms many of the assignments. The constants of most of the lower vibrational states of $HC^{15}NO$ are taken from Ref. (*6*); they are all given in Table I. Transitions from the far infrared, used to determine the constants for the 00012 levels, were taken from the spectra of Refs. (*5, 6*) and are included in Appendix E[1] of this paper.

[1] Appendices comprising 47 tables have been kept on deposit in the Editorial office of the *Journal of Molecular Spectroscopy*. Copies may be obtained from the authors upon request.

The assignment process is done efficiently with an interactive Loomis–Wood assignment program (*15*) and a similarly interactive program to check combination differences. The initial data reduction procedure for the subbands, characterized by a given set of vibrational quantum numbers ($v_1v_2v_3v_4v_5$), a given set of vibrational angular quantum numbers l_4, l_5 and $k = l_4 + l_5$, and a given parity e or f, is to fit each subband separately. A given state is indicated by $v_1v_2v_3v_4^{l_4}v_5^{l_5}$ or $v_1v_2v_3\ (v_4v_5)^k$. Two different combinations of l_4 and l_5 giving the same k are distinguished by a subscript l for the lower and u for the upper of the two levels. The data reduction is done by a program which calculates band centers and effective rotational and centrifugal distortion constants, that is, coefficients in a power series (ps) expansion of the rovibrational term value in $J(J + 1)$,

$$E(J) = G_c + B_{ps}J(J + 1) + D_{ps}J^2(J + 1)^2 + H_{ps}J^3(J + 1)^3 + L_{ps}J^4(J + 1)^4, \quad (1)$$

for both the upper and the lower states. The band center $\tilde{\nu}_c = (G'_c - G''_c)$ is defined as the difference between term values which are thus different from the spectroscopic

TABLE II

Band Centers and Upper State Power Series Constants of Subbands in the ν_2 Band System of $HC^{15}NO$ in cm^{-1}

subband	$\tilde{\nu}_c$	B'_{ps}	D'_{ps} $\times 10^6$	H'_{ps} $\times 10^{12}$	L'_{ps} $\times 10^{15}$	σ $\times 10^4$	lines used
$01000^{0e} \leftarrow 00000^{0e}$	2152.008 81 (20)	0.380 422 5 (22)	0.507 3 (75)	294.6 (96)	-89.2 (40)	4.182	120
$01000^{0e} \leftarrow 00001^{1f}$	1928.590 53 (44)	0.380 421 7 (49)	0.522 (18)	330.1 (240)	-110.8 (110)	2.893	Q 33
$01000^{0e} \leftarrow 00001^{1e}$	1928.590 32 (34)	0.380 417 0 (34)	0.478 (10)	248.2 (110)	-67.6 (40)	6.154	71
$01001^{1f} \leftarrow 00000^{0e}$	2356.591 497 (12)	0.381 768 18 (11)	0.145 13 (30)	-	-	0.1832	Q 46
$01001^{1e} \leftarrow 00000^{0e}$	2356.591 485 (20)	0.380 550 964 (92)	0.139 739 (87)	-	-	0.7388	97
$01001^{1e} \leftarrow 00001^{1e}$	2133.172 19 (27)	0.380 550 470 (83)	0.139 393 (53)	-0.0419 (92)	-	0.9287	109
$01001^{1f} \leftarrow 00001^{1f}$	2133.172 16 (28)	0.381 766 945 (80)	0.144 793 (47)	0.0202 (74)	-	1.0614	120
$01002^{2e} \leftarrow 00001^{1f}$	2393.302 866 (99)	0.381 858 9 (67)	0.158 4 (67)	0.64 (29)	-	0.9553	Q 29
$01002^{2e} \leftarrow 00001^{1e}$	2393.302 953 (32)	0.381 859 05 (14)	0.157 27 (13)	-	-	1.168	69
$01002^{2f} \leftarrow 00001^{1e}$	2393.302 902 (47)	0.381 859 14 (17)	0.139 63 (10)	-	-	0.9664	Q 28
$01002^{2f} \leftarrow 00001^{1f}$	2393.303 007 (24)	0.381 857 93 (11)	0.139 260 (96)	-	-	0.8966	70
$01002^{2e} \leftarrow 00002^{2e}$	2119.342 674 (60)	0.381 858 71 (30)	0.137 94 (29)	-	-	2.373	101
$01002^{2f} \leftarrow 00002^{2f}$	2119.342 83 (10)	0.381 857 61 (68)	0.157 3 (12)	63.8 (67)	-	3.433	105
$01002^{0e} \leftarrow 00000^{0e}$	2669.696 7 (11)	0.382 364 (10)	1.080 (30)	656.6 (320)	-166.9 (110)	19.81	88
$01002^{0e} \leftarrow 00001^{1f}$	2446.275 4 (14)	0.382 426 (15)	1.320 (52)	974.5 (640)	-297.2 (250)	14.20	Q 35
$01002^{0e} \leftarrow 00001^{1e}$	2446.278 36 (90)	0.382 395 (11)	1.226 (37)	869.5 (480)	-256.6 (190)	7.076	39
$01002^{0e} \leftarrow 00002^{0e}$	2129.531 3 (15)	0.382 308 (13)	0.821 (28)	349.5 (210)	-62.1 (48)	55.94	87
$01002^{0e} \leftarrow 0001^{1e}0$	2143.146 3 (12)	0.382 265 1 (95)	0.864 (25)	485.5 (250)	-125.5 (890)	4.621	36
$01003^{1e} \leftarrow 00003^{1e}$	2119.348 134 (98)	0.381 686 47 (80)	0.189 4 (19)	10.0 (16)	-1.02 (44)	2.202	75
$01003^{1f} \leftarrow 00003^{1f}$	2119.347 86 (11)	0.383 439 6 (9)	0.157 4 (25)	6.1 (25)	-1.53 (81)	1.132	56
$01003^{1e} \leftarrow 00001^{1e}$	2765.461 234 (76)	0.381 682 12 (40)	0.176 9 (43)	-	-	1.813	46
$01003^{1f} \leftarrow 00001^{1f}$	2765.460 652 (81)	0.383 436 09 (43)	0.150 72 (45)	-	-	2.180	56
$01003^{3} \leftarrow 00003^{3}$	2109.009 712 (94)	0.382 760 48 (73)	0.145 5 (16)	-8.7 (13)	2.06 (31)	2.126	79
$01004^{4} \leftarrow 00004^{4}$	2102.313 8 (17)	0.383 208 4 (12)	0.157 7 (25)	17.8 (23)	-	1.701	35
$0101^{1e}0 \leftarrow 0001^{1e}0$	2142.643 5 (14)	0.379 672 (12)	-0.606 (28)	-399.2 (230)	77.4 (60)	48.01	91
$0101^{1e}0 \leftarrow 00002^{0e}$	2129.042 5 (13)	0.379 621 (13)	-0.894 (40)	-802.8 (480)	240.9 (190)	10.43	43
$0101^{1e}0 \leftarrow 00001^{1e}$	2445.793 3 (12)	0.379 555 (13)	-1.077 (44)	-995.3 (570)	307.2 (240)	16.76	60
$0101^{1f}0 \leftarrow 0001^{1f}0$	2142.662 013 (27)	0.381 102 61 (25)	0.164 93 (61)	7.77 (54)	-1.14 (15)	0.8330	90
$0101^{1f}0 \leftarrow 00001^{1f}$	2445.807 21 (12)	0.381 106 9 (12)	0.173 7 (40)	20.1 (47)	-5.1 (18)	1.918	67
$0101^{1f}0 \leftarrow 00000^{0e}$	2669.224 04 (10)	0.381 108 82 (86)	0.179 2 (20)	15.9 (13)	-	1.058	Q 23
$01011^{0e} \leftarrow 00011^{0e}$	2123.912 856 (70)	0.381 687 81 (66)	0.429 6 (18)	-1.92 (17)	16.6 (53)	1.625	70
$01011^{0f} \leftarrow 00011^{0f}$	2123.553 404 (44)	0.381 615 22 (32)	0.168 25 (58)	-3.47 (36)	0.95 (7)	1.458	75
$01011^{0f} \leftarrow 0001^{1e}0$	2345.888 68 (37	0.381 621 6 (29)	0.179 2 (50)	-	-	2.878	Q 14
$01011^{2e} \leftarrow 00011^{2e}$	2124.244 08 (12)	0.381 510 5 (11)	-0.173 7 (21)	-33.6 (14)	-2.51 (16)	3.407	58
$01011^{2e} \leftarrow 0001^{1f}0$	2347.794 01 (55)	0.381 510 3 (43)	-0.171 3 (83)	-35.6 (44)	-	8.222	Q 28
$01011^{2f} \leftarrow 00011^{2f}$	2124.243 85 (19)	0.381 521 6 (12)	0.115 3 (19)	7.68 (11)	-2.44 (21)	3.728	81
$01011^{2f} \leftarrow 0001^{1e}0$	2347.794 38 (60)	0.381 521 9 (36)	0.112 3 (44)	-	-	7.671	Q 19
$01012^{3} \leftarrow 00012^{3}$	2111.248 652 (63)	0.382 229 62 (46)	0.117 49 (91)	6.09 (50)	-	1.132	54
$01012^{1e} \leftarrow 00012^{1e}$	2110.955 62 (15)	0.382 452 27 (68)	0.167 07 (68)	-	-	4.985	47
$01012^{1f} \leftarrow 00012^{1f}$	2110.956 83 (11)	0.382 580 50 (64)	0.164 24 (67)	-	-	3.700	52

TABLE III

Band Centers and Upper State Power Series Constants of Subbands in the $2\nu_3$ Band System of $HC^{15}NO$ in cm^{-1}

subband	$\tilde{\nu}_c$	B'_{ps}	D'_{ps} $\times 10^6$	H'_{ps} $\times 10^{12}$	L'_{ps} $\times 10^{15}$	σ $\times 10^4$	lines used
$00200^{0e} \leftarrow 00000^{0e}$	2491.542 05 (21)	0.379 186 3 (13)	0.181 9 (19)	3.37 (97)	0.71 (16)	8.666	107
$00201^{1e} \leftarrow 00001^{1e}$	2502.280 882 (70)	0.379 599 28 (62)	0.146 1 (16)	3.2 (15)	-0.91 (45)	1.754	97
$00201^{1f} \leftarrow 00001^{1f}$	2502.280 878 (27)	0.380 724 72 (17)	0.148 35 (30)	0.18 (14)	-	0.827	97
$00202^{0e} \leftarrow 00002^{0e}$	2501.093 754 (59)	0.380 718 4 (52)	0.121 0 (15)	6.3 (15)	-1.20 (49)	0.841	74
$00202^{2e} \leftarrow 00002^{2e}$	2509.340 99 (40)	0.380 844 8 (68)	0.130 (33)	95.7 (480)	-	2.591	29
$00203^{1e} \leftarrow 00003^{1e}$	2502.477 4 (11)	0.380 289 3 (90)	-0.33 (19)	-	-	4.081	16
$00203^{1f} \leftarrow 00003^{1f}$	2502.472 67 (68)	0.382 146 3 (45)	0.034 (7)	-	-	5.778	24
$00203^{3e} \leftarrow 00003^{3e}$	2514.504 05 (90)	0.381 654 9 (98)	0.276 (31)	214.7 (290)	-	3.775	31
$00211^{1e}0 \leftarrow 00011^{1e}0$	2492.045 780 (41)	0.379 446 4 (39)	0.244 7 (11)	52.6 (12)	-9.12 (38)	0.775	79
$00211^{1f}0 \leftarrow 00011^{1f}0$	2492.045 783 (59)	0.380 207 9 (57)	0.247 3 (16)	49.2 (17)	-9.24 (59)	1.113	73
$00211^{0e} \leftarrow 00111^{0e}$	2503.412 82 (28)	0.380 665 5 (25)	0.534 (66)	67.8 (50)	-	2.830	42
$00211^{0f} \leftarrow 00111^{0f}$	2502.947 17 (15)	0.380 607 5 (17)	0.157 5 (61)	-14.6 (79)	5.7 (33)	1.776	48
$00211^{2e} \leftarrow 00111^{2e}$	2503.224 284 (95)	0.380 521 5 (15)	-0.205 9 (41)	-50.2 (27)	-	4.625	50
$00211^{2f} \leftarrow 00111^{2f}$	2503.224 343 (82)	0.380 524 9 (19)	0.128 7 (51)	4.5 (29)	-	4.761	55
$00212^{1e} \leftarrow 00001^{1e}$	3307.814 81 (16)	0.381 245 56 (92)	0.190 9 (15)	42.76 (87)	-4.48 (16)	4.201	81
$00212^{1e} \leftarrow 00000^{0e}$	3530.850 49 (15)	0.381 232 26 (97)	0.157 2 (17)	17.24 (85)	-	2.044	45
$00212^{1f} \leftarrow 00001^{1f}$	3307.816 91 (38)	0.381 807 5 (27)	-0.003 6 (54)	160.6 (39)	-47.42 (92)	9.467	86
$00212^{1f} \leftarrow 00000^{0e}$	3531.225 43 (38)	0.381 738 1 (36)	-0.129 4 (91)	59.2 (65)	-	3.877	Q 24

TABLE IV

Band Centers and Upper State Power Series Constants of Subbands in the ν_1 Band System of $HC^{15}NO$ in cm^{-1}

subband	$\tilde{\nu}_c$	B'_{ps}	D'_{ps} $\times 10^6$	H'_{ps} $\times 10^{12}$	L'_{ps} $\times 10^{15}$	σ $\times 10^4$	lines used
$10000 \leftarrow 00000$	3333.030 617 (14)	0.381 300 842 (68)	0.158 437 (82)	-0.908 (26)	-	0.576	95
$10000^{0e} \leftarrow 00001^{1e}$	3109.613 881 (64)	0.381 300 59 (36)	0.158 91 (44)	-	-	1.410	52
$10000^{0e} \leftarrow 00001^{1f}$	3109.613 901 (61)	0.381 299 45 (45)	0.157 76 (94)	-1.21 (56)	-	0.785	Q 35
$10001^{1e} \leftarrow 00000^{0e}$	3529.104 20 (11)	0.381 696 2 (13)	0.187 1 (41)	-33.4 (49)	9.3 (19)	2.325	73
$10001^{1e} \leftarrow 00001^{1e}$	3305.687 581 (69)	0.381 693 96 (79)	0.184 3 (27)	-33.7 (34)	8.4 (14)	1.320	65
$10001^{1f} \leftarrow 00001^{1f}$	3305.687 727 (74)	0.382 798 6 (10)	0.295 4 (44)	-166.1 (71)	49.5 (36)	1.055	55
$10002^{2e} \leftarrow 00001^{1e}$	3557.245 528 (64)	0.383 237 85 (35)	0.166 78 (40)	-	-	1.550	39
$10002^{2e} \leftarrow 00001^{1f}$	3557.245 558 (76)	0.383 236 38 (33)	0.166 10 (27)	-	-	1.634	Q 31
$10002^{2f} \leftarrow 00001^{1f}$	3557.245 552 (91)	0.383 236 24 (51)	0.146 36 (57)	-	-	2.392	44
$10002^{2f} \leftarrow 00001^{1e}$	3557.245 21 (12)	0.383 238 43 (47)	0.147 55 (35)	-	-	1.621	Q 24
$10002^{2e} \leftarrow 00002^{2e}$	3283.287 97 (14)	0.383 235 40 (63)	0.165 09 (60)	-	-	4.347	77
$10002^{2f} \leftarrow 00002^{2f}$	3283.287 78 (11)	0.383 236 89 (51)	0.146 18 (46)	-	-	4.023	76
$10002^{0e} \leftarrow 00002^{0e}$	3292.996 603 (24)	0.382 897 81 (12)	0.128 69 (12)	-	-	0.771	77
$10003^{3e} \leftarrow 00002^{2f}$	3571.301 73 (15)	0.383 749 8 (14)	0.185 7 (29)	-	-	1.919	Q 17
$10003^{3e} \leftarrow 00002^{2e}$	3571.301 29 (23)	0.383 753 3 (30)	0.207 8 (82)	-	-	2.429	14
$10003^{3f} \leftarrow 00003^{3f}$	3257.672 738 (91)	0.383 752 7 (77)	0.195 0 (18)	-6.3 (15)	1.56 (41)	2.165	67
$10003^{3f} \leftarrow 00003^{3e}$	3257.672 90 (75)	0.383 750 6 (82)	0.199 (18)	-	-	10.51	Q 16
$10003^{1e} \leftarrow 00003^{1e}$	3275.327 395 (99)	0.382 514 60 (50)	0.119 47 (46)	-	-	2.397	36
$10003^{1f} \leftarrow 00003^{1f}$	3275.327 550 (83)	0.384 481 30 (42)	0.131 12 (40)	-	-	2.246	40
$10004^{4e} \leftarrow 00004^{4e}$	3239.317 513 (92)	0.384 295 47 (45)	0.161 35 (48)	-	-	1.549	50
$10004^{2e} \leftarrow 00004^{2e}$	3247.317 61 (38)	0.383 916 6 (28)	0.276 0 (44)	-	-	7.499	33
$10004^{2f} \leftarrow 00004^{2f}$	3247.317 80 (41)	0.383 905 1 (31)	0.152 6 (49)	-	-	7.937	32
$10011^{1e}0 \leftarrow 00011^{1e}0$	3329.417 16 (33)	0.381 386 1 (31)	0.161 0 (76)	-15.2 (54)	-	4.925	42
$10011^{1f}0 \leftarrow 00011^{1f}0$	3329.414 82 (31)	0.382 102 4 (28)	0.232 1 (69)	42.6 (48)	-	4.477	45
$10011^{0e} \leftarrow 00111^{0e}$	3302.618 51 (15)	0.382 873 3 (12)	0.607 6 (25)	57.9 (14)	-	3.065	45
$10011^{0f} \leftarrow 00111^{0f}$	3302.222 53 (12)	0.382 727 67 (52)	0.237 79 (43)	-	-	4.070	50
$10011^{2e} \leftarrow 00111^{2e}$	3302.347 19 (41)	0.382 492 4 (47)	-0.249 (15)	-101.0 (130)	-	6.835	43
$10011^{2f} \leftarrow 00111^{2f}$	3302.347 29 (26)	0.382 502 9 (30)	0.124 4 (84)	-65.9 (61)	-	4.773	38
$10012^{3} \leftarrow 00012^{3}$	3279.785 19 (24)	0.383 526 8 (23)	0.103 5 (51)	-6.5 (30)	-	5.816	55
$10012^{1e} \leftarrow 00012^{1e}$	3280.402 70 (24)	0.383 685 3 (22)	0.228 7 (52)	20.7 (41)	-4.7 (10)	5.800	52
$10012^{1f} \leftarrow 00012^{1f}$	3280.405 46 (31)	0.383 773 8 (14)	0.193 6 (16)	-	-	3.096	50

TABLE V

Band Centers and Upper State Power Series Constants of Subbands in the $\nu_2 + \nu_3$ Band System of $HC^{15}NO$ in cm^{-1}

subband	$\tilde{\nu}_c$	B'_{ps}	D'_{ps} $\times 10^6$	H'_{ps} $\times 10^{12}$	L'_{ps} $\times 10^{15}$	σ $\times 10^4$	lines used
$01100^{0e} \leftarrow 00000^{0e}$	3387.485 33 (20)	0.378 835 5 (13)	0.075 6 (23)	−20.4 (14)	8.87 (26)	7.303	89
$01100^{0e} \leftarrow 00001^{1f}$	3164.068 24 (39)	0.378 847 3 (36)	0.109 1 (94)	10.5 (73)	-	2.496	Q 17
$01101^{1e} \leftarrow 00001^{1e}$	3374.023 00 (36)	0.379 053 8 (17)	0.123 5 (17)	-	-	9.456	47
$01101^{1f} \leftarrow 00001^{1f}$	3374.022 99 (24)	0.380 262 4 (21)	0.107 6 (47)	−14.8 (29)	-	3.937	39
$01102^{2e} \leftarrow 00002^{2e}$	3366.639 8 (19)	0.380 247 (21)	-0.435 (72)	-526. (88)	166. (35)	26.75	57
$01102^{0e} \leftarrow 00002^{0e}$	3372.675 81 (22)	0.380 243 5 (31)	0.047 (13)	−95.2 (190)	76.4 (94)	3.405	45
$0111^{1e}0 \leftarrow 0001^{1e}0$	3379.039 53 (12)	0.379 033 9 (12)	0.092 5 (35)	−6.9 (38)	7.7 (13)	2.117	64
$0111^{1f}0 \leftarrow 0001^{1f}0$	3379.040 12 (15)	0.379 784 85 (70)	0.092 98 (64)	-	-	4.382	59
$01111^{0e} \leftarrow 00011^{0e}$	3365.922 5 (85)	0.380 252 4 (84)	0.628 (23)	145.4 (190)	-	11.46	32
$01111^{0f} \leftarrow 00011^{0f}$	3365.375 37 (30)	0.380 133 4 (15)	0.147 3 (16)	-	-	5.260	32
$01111^{2e} \leftarrow 00011^{2e}$	3366.105 3 (12)	0.380 101 (14)	-0.089 (23)	-	-	19.33	19
$01111^{2f} \leftarrow 00011^{2f}$	3366.112 3 (24)	0.380 031 (15)	0.024 (23)	-	-	46.26	23

term value G_v (*8*) which is defined by band origins. When the lower state had been identified, the constants for the lower state were held fixed at the values given in Table I while constants of the upper state were determined. The expression in Eq. (1) cannot describe a complete k polyade of an excited state simultaneously. The power series coefficients provide only a nearly "model-free" representation of the term values. They are a check of the vibrational assignment, but are not directly related to a molecular Hamiltonian.

In earlier papers reporting data for fulminic acid and its isotopomers we have fit all the data with an effective Hamiltonian for linear molecules (*8*). In contrast to the situation in the far IR, this ansatz gives satisfactory results in only a few exceptional cases, for states with term values about 2000 cm^{-1}. The perturbations observed here are so numerous, that it was not possible to determine physically significant constants in the Hamiltonian for more than a fraction of the bands reported here. Even where we have identified the resonances, a suitable Hamiltonian would require the simultaneous fit of transitions to several states with various l multiplets. We have for the time being limited ourselves to extracting physical information from the band centers and B_{ps} values. Even relying on the simple analysis based on Eq. (1), the density of states in the range of energy investigated is already so large that resonances with normally "dark" states distort the bands, leading to deviations up to 100 times the experimental standard deviation σ.

The constants obtained for the upper states involved in the rovibrational transitions of the ν_1, ν_2, $2\nu_3$, and $\nu_2 + \nu_3$ band systems so far assigned are given in Tables II–V. The complete list of line positions of the assigned rovibrational transitions is given in Appendices A–D in a sequence corresponding to Tables II–V. The fit procedure used a relative weighting factor w for every line with $w = (1 - \text{transmittance})^2$, thus giving a very low weight to the far wings of the bands. Therefore in some perturbed bands, large deviations are found for lines with high J values.

The combination of the effects of accidental resonances and irregularities resulting from the quasilinearity of the ν_5 manifold leads to a complex spectrum. Many of the bands show localized rotational perturbations; an example of a global Coriolis perturbation of entire bands is presented below. The spectra of HCNO and its isotopomers also show a pattern of Fermi resonances (*6*). There is almost no band that is free of resonance effects. The constants in Tables II–V are affected by all the known and

unknown resonances, although we have excluded from the fit lines obviously perturbed by local resonances. In Table VI we list the states identified so far, their term values as defined by Eq. (1), and comments concerning perturbed states. The horizontal lines in Table VI delineate interacting groups of levels. As yet no systematic assignment of the partners in the local resonances has been attempted, although several have been identified.

"FORBIDDEN" BANDS

As already noted, there are many resonances in the spectrum of $HC^{15}NO$. In Fig. 1 a box around the interacting terms shows a prominent resonance found in the spectrum. A Coriolis resonance between the states $0101^{1e}0$ and 01002^{0e} gives rise to several normally forbidden bands, or more rigorously, Coriolis-allowed transitions. The centers of the bands arising from the terms in resonance have a separation of 0.5 cm^{-1}. The transitions $0101^{1e}0 \leftarrow 00002^{0e}$ and $01002^{0e} \leftarrow 0001^{1e}0$, which actually acquire intensity due to a Coriolis interaction both in the lower state (small effect) (6) and in the upper state (dominant effect), were found. They are shown in Fig. 2 as diagonal arrows which are omitted in Fig. 1. The subbands involved show especially obvious deviations in the power series fits.

Figure 3 displays in a Loomis–Wood diagram one band of this resonance, the hot band $0101^{1e,f}0$–$0001^{1e,f}0$, in which the e component shows the effect of the $0101^{1e}0$/

TABLE VI

Term Values Determined or Estimated for $HC^{15}NO$ in cm^{-1}
(States in the Same Box May Be in Resonance)

STATE	G_c	INTERACTIONS	STATE	G_c	INTERACTIONS
00015^0	2158 ??		10001	3529.104	str.r.
01000	2152.015	gl.r.	$002(12)^{1f}$	3531.225	str.r.
01001	2356.591		01101	3597.440	l.r.J=12, str.l.r.J=15/16
00200	2491.542	gl.r., l.r. J=47	10002^2	3780.662	
01002^2	2616.720		10002^0	3833.158	
01010	2669.224	Coriolis gl.r.	10010	3855.979	
01002^0	2669.697	without crossing	01102^2	3864.006	gl.r., str.l.r. J=13
00201	2725.698	l.r. J=27	01110	3905.602	
$010(11)^{0e}$	2871.024		01102^0	3912.837	l.r. J=31
$010(11)^{0f}$	2872.450		$100(11)^{0e}$	4049.730	
$010(11)^2$	2874.355	gl.r.	$100(11)^{0f}$	4051.120	
01003^3	2920.012	l.r. J=34	$100(11)^2$	4052.458	l.r. J=21
01003^1	2988.878		10003^3	4068.675	l.r. J=24
00202^2	3006.715	str.gl.r., l.r. J= 29	$011(11)^{0e}$	4113.038	l.r.
00210	3018.608	l.r. J=18	$011(11)^{0f}$	4114.272	l.r.
00202^0	3041.255	l.r. J=42	$011(11)^2$	4116.566	str.l.r. J=13
$010(12)^{1f}$	3131.326		10003^1	4144.856	
$010(12)^3$	3136.109		$100(12)^{1f}$	4300.774	
$002(11)^{0e}$	3250.524		$100(12)^3$	4304.645	gl.r.
$002(11)^{0f}$	3251.844		1002^20	4378.201	
$002(11)^2$	3253.355		10004^4	4397.131	
01004^4	3260.127		10004^2	4469.060	
00203^3	3325.506	gl.r.			
10000	3333.031	weak gl.r.			
00203^1	3371.999				
01004^0	3383. ??				
01100	3387.485	str.r., l.r. J=30, 48			

str: strong, gl: global, l: local, r: resonance,
??: expected value

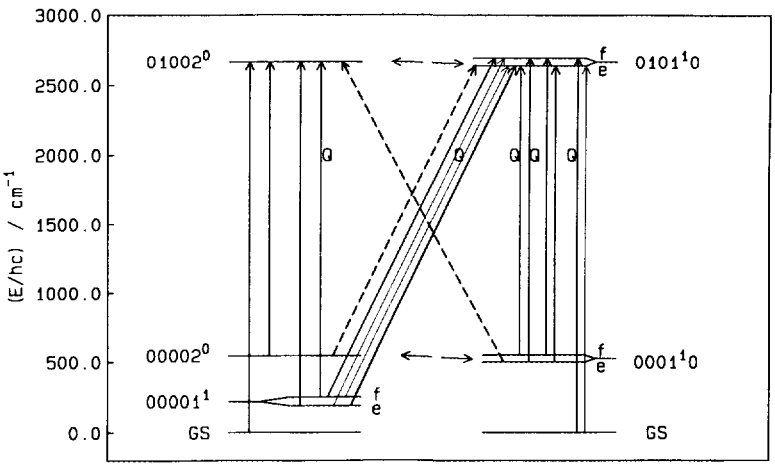

FIG. 2. Transitions connecting the interacting levels 00010/00002 and 01010/01002 in HC^{15}NO. Full lines show allowed transitions. The thin lines indicate transitions which are allowed, but not seen. The solid diagonal arrows involving the *e* levels in the upper state are resonance enhanced, while broken diagonal arrows are Coriolis resonance-induced transitions.

01002^{0e} interaction. The difference band $0101^{1e,f}0 \leftarrow 00001^{1e,f}$ must be classified as resonance enhanced for the *e* component, since even the *f* component, which is unaffected by either resonance, could be seen. However, the *P* branch of the *e* component is a factor of roughly 1.8 stronger and the *R* branch of the *e* component is the same factor weaker than the *f* component, as a result of resonance enhancement/depletion of the transition moment.

A plot of the reduced rovibrational term values for the transitions to the upper states $0101^{1e}0$ and 01002^0 from $J = 1$ to $J = 60$, reproduced in Fig. 4, shows that no crossing of the term values of these states takes place. This is in contrast to the pattern

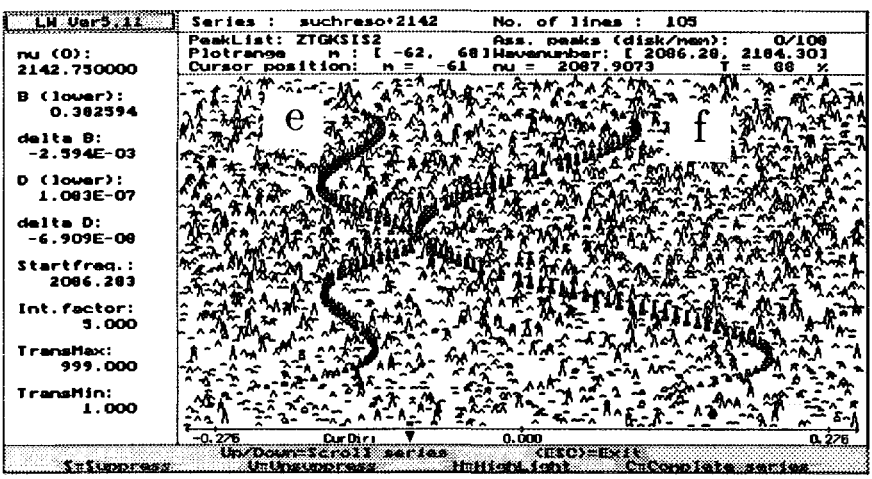

FIG. 3. Coriolis perturbed (e) and unperturbed (f) components of the $0101^{1e,f}0$–$0001^{1e,f}0$ subbands in HC^{15}NO in a Loomis–Wood program screen dump.

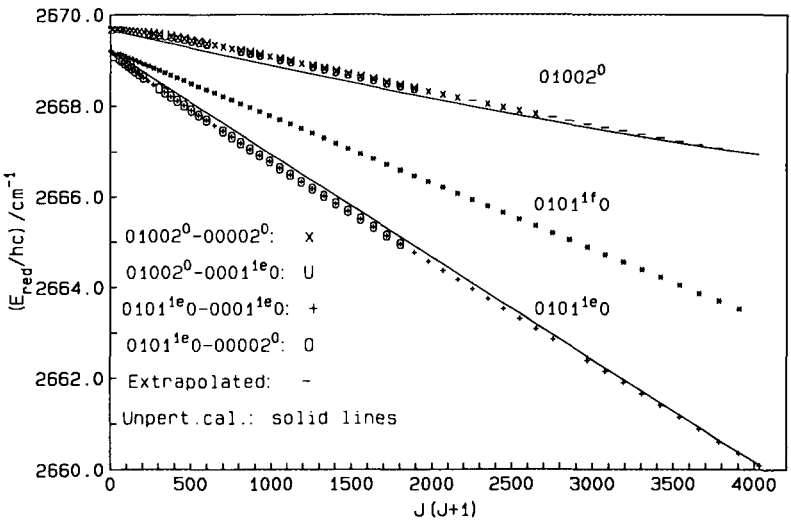

FIG. 4. Reduced term values of the 01010/01002 levels of HC^{15}NO. The full lines are unperturbed levels calculated with the Coriolis resonance coefficient set to zero.

of the 00010^{1e}/00002^{0e} resonance in H^{13}CNO, where the analogous unperturbed levels cross (*4*). However, since the divergence of the unperturbed levels is slow, and the interaction matrix element increases with J, it is a global perturbation of both states, for all observed J values. The observed reduced term values were obtained using the Ritz combination principle. The unperturbed calculated curves in Fig. 4 are calculated with the adjusted set of fitted constants, determined from the effective Hamiltonian including the resonance as in Ref. (*4*) for both upper and lower states, but with the Coriolis coupling constant set to zero.

Figure 5 shows a plot of the absorbtance values of some of the transitions to the interacting levels indicated in Fig. 2. The plot shows an equal absorbtance for both of the allowed hot bands, which is to be expected, since the Bolzmann factor for the two bands is indistinguishable. Similarly, the plot shows an equal absorbtance of the two resonance-allowed transitions, which are rather weak relative to the allowed hot bands: they are probably a factor of 10 weaker than the allowed hot bands. This is consistent with the information revealed by Fig. 4: The shift of the term values is only moderate, so the mixing of the levels leads to only weakly allowed resonance-induced transitions. It is to be noted, especially, that P and R branches are equally intense in the resonance-allowed bands. This indicates (see the discussion in Ref. (*4*)) that the transition moments for the unperturbed transitions 01002 ← 00010 and 01010 ← 00002 are effectively zero. This again is in contrast to the situation found in Ref. (*4*), and to that of the difference band 0101 ^{1e}0 ← 00001 ^{1e}, mentioned above.

A further obvious resonance system involves the 10001 ^{1} state. Two bands of nearly equal strength appear in the region of both the hot band 10001 ^{1} ← 00001 ^{1}, near 3306 cm^{-1}, and the combination band 10001 ^{1} ← 00000, near 3531 cm^{-1}, involving both e and f components. These four bands define a resonance for the upper state, 10001 ^{1}, which does not have a counterpart in the parent species. The tentative assignment of the interacting level is 002(12)^{1e,f} or 002(1 ^{1}2^{-2}). Figure 6 is a plot of the reduced rovibrational term values for the upper state. It can be interpreted as showing crossings of the term values for the f components near $J \approx 30$ and at higher J (>40) for the

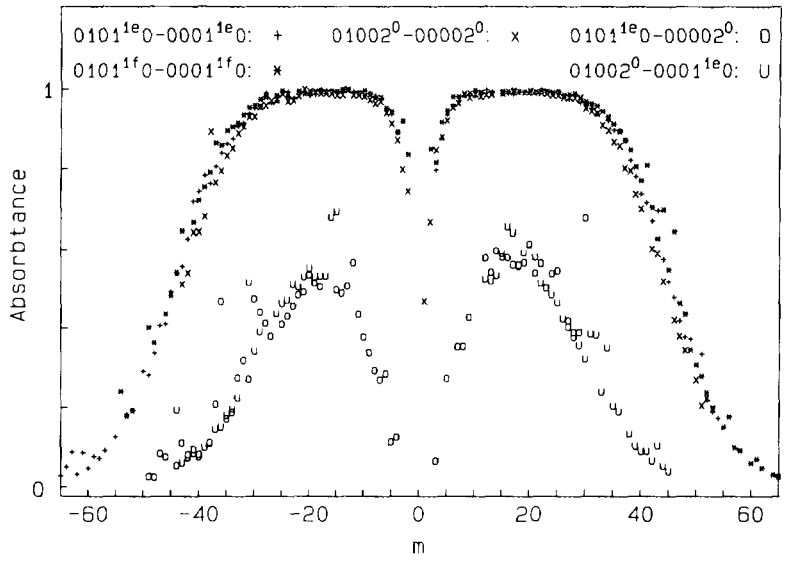

FIG. 5. Absorbtance of the 01010/01002 hot band system in HC^{15}NO. The absorbtance values are plotted versus the index m, where $m = -J$ in the P branch and $m = J + 1$ in the R branch.

e components. The identification indicates the nature of many of the interactions which we have to consider: in particular, high excitation of one or both bending modes.

Numerous further subbands, for which we could not yet find a reliable vibrational assignment, have also been observed. We hope to assign some of them on the basis of improved predictions of "dark" states.

DISCUSSION

Figure 7 shows the term values of the anharmonic HCN bending mode ν_5 of HC^{15}NO as a function of the excitation of the remaining vibrational modes. The CH stretch ν_1

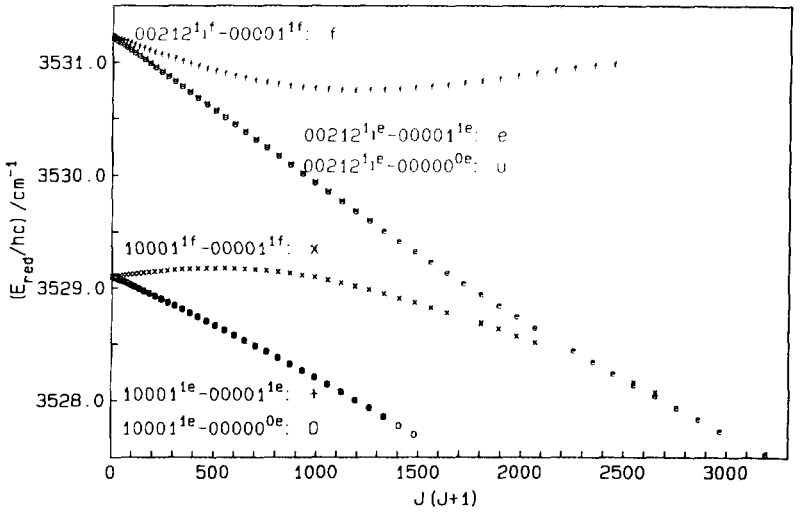

FIG. 6. Reduced term values of the 10001/00212 levels of HC^{15}NO.

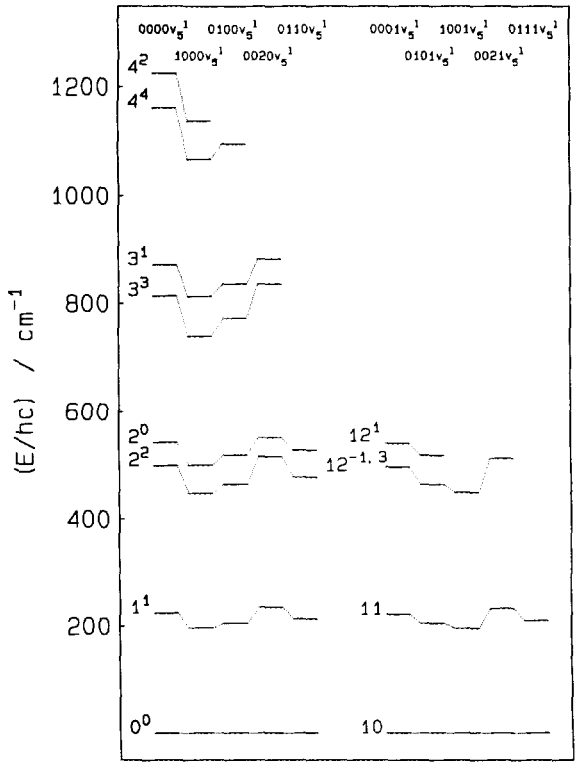

FIG. 7. Dependence of the term value intervals in the ν_5 manifold on the other modes in HC^{15}NO.

has the strongest influence on the HCN bending levels, lowering the vibrational manifold and increasing the splitting, i.e., increasing the quasilinear character of the ν_5 stack. This indicates an increase of the barrier height in the HCN bending potential upon excitation of the C–H stretching mode. The excitation of the NO stretch overtone $2\nu_3$ leads on the other hand to a slight upward shift in energy of the HCN bending levels. Thus, excitation of this latter mode decreases the quasilinear character of the molecule. The shifts per quantum of ν_3 are found to be larger if ν_2 is excited; in a slightly anharmonic model, this would indicate a nonzero value of x_{23}. The anharmonic intervals and shifts summarized in Fig. 7 correspond roughly to those found from more limited data for the parent species (*9*). They indicate why it is difficult to extrapolate upwards to identify resonance partners in this molecule.

Figure 8a shows large and very nonlinear variations of the rotational constant B_{ps} as a function of the excitation of the bending vibrational mode ν_5 and of the other modes. The reduced presentation emphasizes the deviation of the B values in HC^{15}NO from the linear expansion for the harmonic case

$$B_v = B_e - \sum_i \alpha_i (v_i + d_i/2). \tag{2}$$

These deviations parallel the effects shown in Fig. 7. We report in Fig. 8b a similar summary for the l-type doubling constant q_5, which describes the splitting of the $l = 1$ levels according to

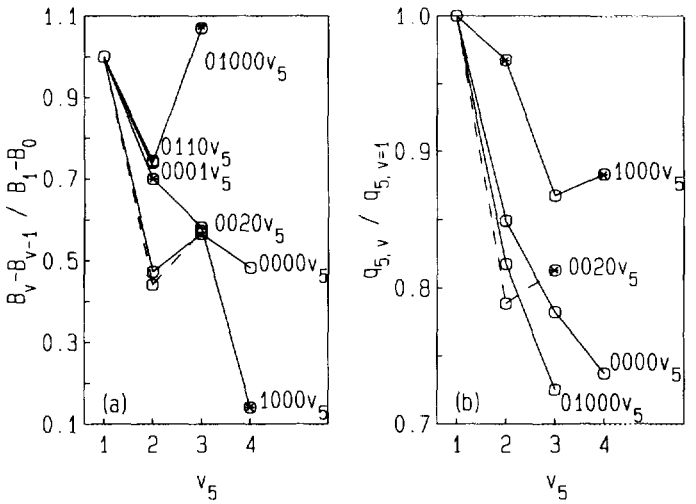

FIG. 8. Dependence of (a) the rotational constants B_{ps} and (b) the l-type doubling constant q_5 on the bending quantum number v_5 in different vibrational states of $HC^{15}NO$. For $l > 0$, the average of B_{ps} for the e and f values is plotted. Asterisks indicate values derived for perturbed levels, which fall out of the general pattern.

$$\Delta E = \tfrac{1}{2} q_5(v_5 + 1)J(J + 1). \tag{3}$$

For $v_5 = 2$ and 4, values of q_5 were obtained from fits to the effective Hamiltonian (*3, 8*), which, as noted above, were otherwise of limited value. As can be seen, this quantity is not nearly constant, as would be expected for a linear molecule, but changes by 20% from the first to the third excited state.

An overview of the spectrum of $HC^{15}NO$ is given in Figs. 9 and 10. Many of the bands reported here can be identified in these spectra with the aid of band centers listed in Tables II–V. Some transitions are indicated with an assignment comb. Because of the chemical instability of $HC^{15}NO$ the isomerization product $H^{15}NCO$ is also present. Also, 10% of the sample is the main species HCNO, while $H^{13}C^{15}NO$ is present in the natural abundance of ^{13}C ($\sim$1%), both of which contribute observable bands. CO_2 is also observable.

The intercomparison of the spectra of HCNO and $HC^{15}NO$ has aided assignments in both spectra. When more of the resonances have been analyzed, a comprehensive picture of the energy levels and resonances can be filled in for both species.

Since the nitrogen nucleus in fulminic acid lies nearly at the center of gravity, one expects that the species $HC^{15}NO$ should behave quite similarly to HCNO rotationally, but not necessarily vibrationally, especially for modes involving the nitrogen. The ν_1 transitions and their combination bands and hot bands in the four species HCNO, $HC^{15}NO$, $H^{13}CNO$, and $H^{13}C^{15}NO$ lie near each other and are very similar. The most striking difference between these bands in $HC^{15}NO$ and HCNO is the strong resonance pattern of the 10001 state, discussed above, which is brought into resonance by the ^{15}N isotope shift of the 00212 state. The transitions of hot bands of the ν_2 combination states in which a CN vibration is excited are shifted downward in wavenumber in the ^{15}N species by ca. 44 cm^{-1}. The downward shift of the ν_2 levels and the shift in ν_4 relative to $2\nu_5$ lead to an accidental separation of less than 1 cm^{-1} for the resonance system $(02)^0$ and $(10)^{1e}$ in combination with ν_2. In the spectra of the

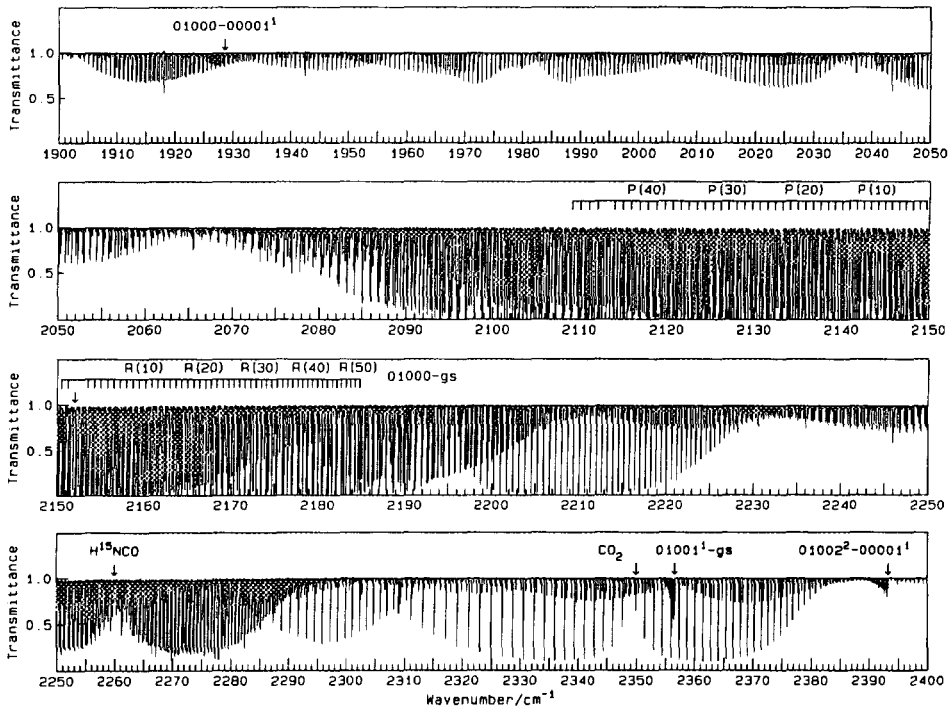

FIG. 9. Spectrum of $HC^{15}NO$ in the range 1900–2400 cm^{-1}.

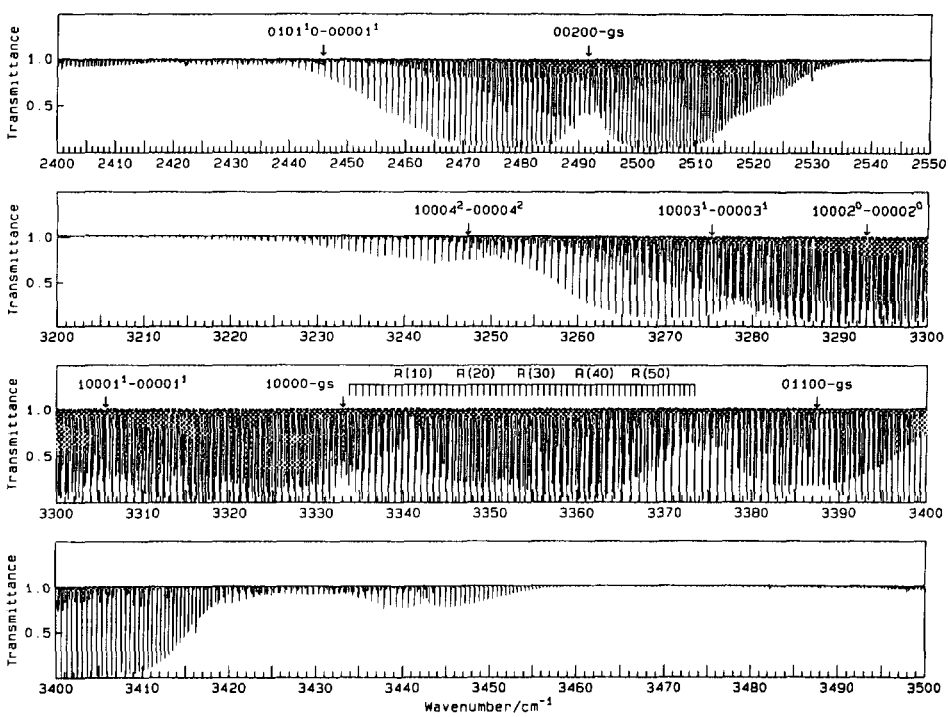

FIG. 10. Spectrum of $HC^{15}NO$ in the range 2400–3500 cm^{-1}.

other isotopomers this particular resonance system is only weak. Thus, a change from one isotopomer to another gives us a "tuning" of every resonance.

ACKNOWLEDGMENTS

We thank Dr. R. Wilmes for preparing the precursors for the $HC^{15}NO$, and K. Lattner for his help in recording the spectra. G. Wagner is thanked for providing the precise values of ground state constants (6), for making the transitions to the 00012 states available, and for helpful discussions on assignments and resonances. For financial support we thank the Deutsche Forschungsgemeinschaft and the Fonds der chemischen Industrie.

RECEIVED: March 3, 1993

REFERENCES

1. C. WENTRUP, G. GERECHT, AND H. BRIEHL, *Angew. Chem.* **91,** 503–504 (1979).
2. B. P. WINNEWISSER, M. WINNEWISSER, AND F. WINTER, *J. Mol. Spectrosc.* **51,** 65–96 (1974).
3. B. P. WINNEWISSER, M. WINNEWISSER, G. WAGNER, AND J. PREUSSER, *J. Mol. Spectrosc.* **142,** 29–56 (1990).
4. G. WAGNER, B. P. WINNEWISSER, AND M. WINNEWISSER, *J. Mol. Spectrosc.* **146,** 104–119 (1991).
5. G. WAGNER, B. P. WINNEWISSER, M. WINNEWISSER, AND K. SARKA, to be published.
6. G. WAGNER, "Dissertation," Justus-Liebig-Universität Giessen, 1991, and private communication.
7. F. IACHELLO, N. MANINI, AND S. OSS, *J. Mol. Spectrosc.* **156,** 190–200 (1992).
8. K. M. T. YAMADA, F. W. BIRSS, AND M. ALIEV, *J. Mol. Spectrosc.* **112,** 347–356 (1985).
9. B. P. WINNEWISSER, *in* "Molecular Spectroscopy: Modern Research" (K. Narahari Rao, Ed.), Vol. III, Chap. 6, Academic Press, New York, 1985.
10. G. GUELACHVILI AND K. NARAHARI RAO, "Handbook of Infrared Standards," Academic Press, New York, 1986.
11. J.-I. CHOE, T. TIPTON, AND G. KUKOLICH, *J. Mol. Spectrosc.* **117,** 292–307 (1986).
12. B. P. WINNEWISSER, *J. Mol. Spectrosc.* **40,** 164–176 (1971).
13. E. L. FERETTI AND K. NARAHARI RAO, *J. Mol. Spectrosc.* **51,** 97–106 (1974).
14. S. ALBERT, "Diplomarbeit," Justus-Liebig-Universität Giessen, 1991.
15. B. P. WINNEWISSER, J. REINSTÄDTLER, K. M. T. YAMADA, AND J. BEHREND, *J. Mol. Spectrosc.* **136,** 12–16 (1989).
16. P. JENSEN, *J. Mol. Spectrosc.* **101,** 422–439 (1983).
17. J. K. HOLLAND, D. A. NEWNHAM, I. M. MILLS, AND M. HERMANN, *J. Mol. Spectrosc.* **151,** 346–368 (1992).